

Glass clarified as the Self-Organizing System

Elena A. Chechetkina

Institute of General and Inorganic Chemistry of Russian Academy of Sciences (1980-2011)

Moscow, Russia

eche2010@yandex.ru

Abstract – The term “self-organization” in a contemporary glass science relates usually to “intermediate phase” in frames of the *topological constraint theory* of glass structure. This theory, however, has no a relation to classical theory of self-organization – synergetics. The synergetic approach proposed here is based on characteristic instability of chemical bonding in the form of the *bond wave* considered as the spatiotemporal correlation between the elementary acts of bond exchange. In frames of the model, glass transition represents the *dimensionality transition*: from the 3D bond wave in glass-forming liquid to the 2D bond wave in glass. By using of available experimental data, the bond wave model displays *non-crystalline long-range order*, *semi-deterministic behavior of viscosity*, and *information field* as a necessary condition for glass formation.

Keywords: *glass, self-organization, chemical bonding, glass transition, glass structure, glass-forming liquid, viscosity, fractography, information field*

I. INTRODUCTION

Glass articles accompany us everywhere – from windows and kitchenware to fiber communications and active elements for electronic devices. At the same time no one material is so enigmatic, when even the nature of glass transition remains a subject of incessant discussions. To my opinion, the scientific mist appears because of ignoring of self-organization, a widespread phenomenon observed everywhere: in physics, chemistry, biology, psychology, sociology, etc. [1-3].

My understanding glass as the self-organizing system began in 1980s in the laboratory of *S. A. Dembovsky*, who was creating a new theory of glass formation based on the chemical bond point of view. The core of his theory are special bonds in the form of *hypervalent bonds*, which were considered initially as “defects” in covalent network [4] and after as a necessary element of glass structure, an element that ensures both glass properties and glass formation phenomenon at all [5]. During rummage of the “glassy” bonds by experiments of viscous flow in magnetic fields [6,7] my bond wave model was born.

Bond wave is considered as the spatiotemporal correlation between the bond transformation acts. The model was successively applied then for explanation of other glass features, both the known ones (medium-range order, non-Arrhenius behavior of viscosity, specific fracture) and those discovered by action of weak *information fields* (magnetic,

ultrasound, etc.). The bond wave model history, present state and future development are considered in this paper.

II. DISSIPATIVE PATTERN – THE BOND WAVE

Glass is understood usually as the *bulk non-crystalline material obtained by cooling from melt and then supercooled liquid up to complete solidification* [8,9]. Corresponding process is shown schematically in **Fig.1**, where T_g , T_m , T_b , and T_m^* are the glass transition temperature, melting point, boiling point, and the “normal” melting point (see comments to **Table 1**).

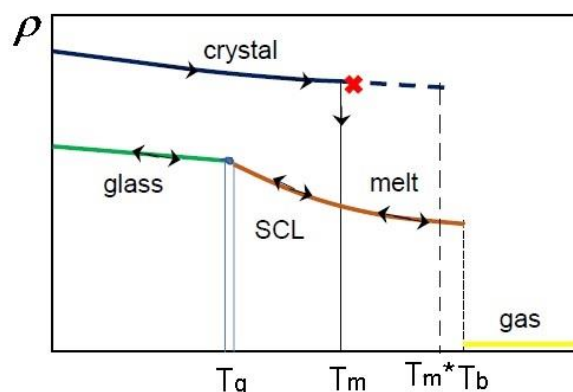


Figure 1. Density-temperature diagram for the crystal-melt-glass transformations; SCL is supercooled liquid.

Typical inorganic glasses belong to oxides (SiO_2 , B_2O_3 , etc.) or chalcogenides (Se , As_2S_3), both groups being based on **covalent bonds**, e.g., Si–O for SiO_2 or As–S for As_2S_3 . Conventional **continuous random network (CRN)** model of glass structure [10] operates with the same covalent bonds in glass and crystal. For example, each O-atom of SiO_2 forms two covalent bonds with its neighbors, so being *two-coordinated* (O_2), and each Si-atom is *four-coordinated* (Si_4). This means that CRN operates with the **short-range order (SRO)**, and there is no a difference between SRO in glassy and crystalline states of a substance.

Classical CRN (**Fig.2a**) corresponds to the B_2O_3 -like network consisting of B_3 and O_2 atoms. Such a CRN, however, cannot realize “in bulk” because of characteristic *rigidity* of covalent bond, which can change the bond length and valence angles only in narrow limits, a fact that makes classical CRN unstable after few random conjunctions.

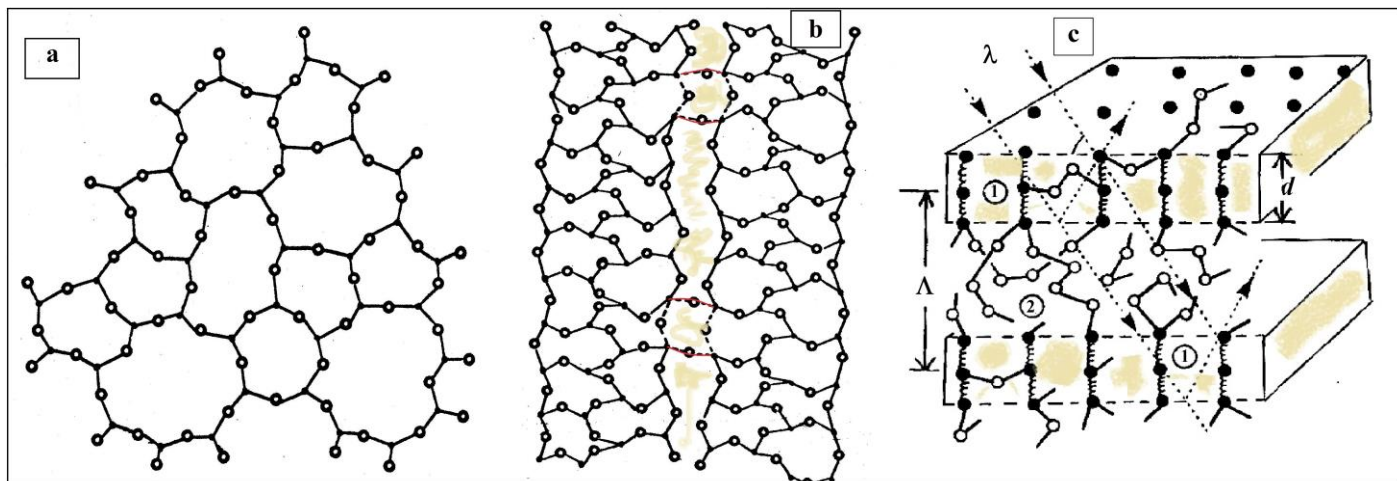


Figure 2. Models for glass structure after (a) *Zachariasen* [10], (b) *Robinson* [11] and (c) *Chechetkina* [12].

To overcome this shortcoming, *Robinson* [11] has introduced into CRN the “cuts” populated with weak/flexible bonds (**Fig.2b**), thus tailoring rigid covalent fragments with the following increase of CRN stability. Note that the notions about some “*weak bonds*” emerge periodically in glass literature (see, e.g., Ref.13); however, without appropriate justification of the bonds’ nature.

Two other ways for reconstruction of classical CRN concern either special junction of covalent bonds such as “*outrigger rafts*” after *Phillips* [14] or the **topological constraint theory** of glass structure [15-17]. The theory considers only “normal” atomic coordination (i.e., Si₄, O₂, As₃, Se₆, etc.) which are used for calculation of the *average coordination number* $\langle r \rangle$ in accord with chemical composition of a system. The obtained $\langle r \rangle$ is compared with “*magic*” coordination number $\langle r \rangle^* = 2.4$ which corresponds to the free-of-stress state of a network. Really, the composition-property dependencies in binary glass-forming systems demonstrate anomaly in the region around corresponding “*magic*” composition; just this “*intermediate phase*” [18] is compared with the *self-organization* phenomenon in glass.

To my opinion, self-organization is a basic feature of the glassy state irrespectively of chemical composition. The bond wave model naturally combines “*weak bonds*” and “*self-organization*” owing to the *two-state* chemical bonding and a collective *feedback* between the states in the form of the **bond wave** representing the spatiotemporal correlation between elementary acts of reversible transformation between basic covalent bond (CB) and exited **alternative bond (AB)**: $\Sigma\Sigma(\text{CB} \leftrightarrow \text{AB})$, no matter now what is the AB nature.

The bond wave “*elementary cell*” is shown in **Fig.2c**, where alternative bonds are considered as the three-center bonds (TCB) in accord with the early model of hypervalent bonds after *Dembovsky* [4]. The following quantum-chemical study of “*glassy*” bond revealed concrete hypervalent bonds in

typical glass formers (see review [5]); however, the nature of AB is of no matter now, as well as the network motive: 1D (like Se), 2D (like B₂O₃) or 3D (like SiO₂).

From a historical point of view, the bond wave model was born in the middle of 1980s owing to our magneto-viscous experiments [6,7], whose features – the field weakness and diamagnetic nature of glass – cannot be explained in frames of classical physics. Fortunately, the self-organization notions developed intensively at that time, but unfortunately, not in glass science, a fact that forced me to choose a roundabout way to meet glass community with the bond wave idea.

In doing so, I have used common thermodynamic data, phase transitions temperatures (T_m and T_b) and atomization energy (E_a), for construction of the $T_m=f(E_a)$ and $T_b=f(E_a)$ plots for “*normal*”, molecular, and glass-forming substances [19]. Molecular substances, as expected, fall far below the “*normal*” lines. The fall of glass-formers is much less but remains strong enough to be neglected. For example:

Table 1. Atomization energy and phase transition temperatures for Se and SiO₂: real (T_m and T_b) and “*normal*” (T_m^* and T_b^*)

	E_a , kcal/g-at	T_m , K	T_m^* , K	T_b , K	T_b^* , K
Se	52	494	940	958	1550
SiO ₂	149	1883	2700	2503	4400

This fact points to a substantial *inhomogeneity* in chemical bonding for two falling groups. Molecular substances are composed of strong covalent bonds within the molecules and very weak van-der-Waals bonds acting between them, so even a light heating leads to destruction of a molecular crystal; firstly at T_m , above which the temporarily closing molecules are linked with van-der-Waals bonds that switch from some atoms to others, and then at T_b , when van-der-Waals bonds break totally releasing free molecules into the gaseous phase.

The covalently bonded crystal endures thermal stress longer, up to a relatively high “normal” temperature T_m^* , above which the system of covalent bonds destroys totally because of metallization. Ideal metallic bond represents the positively charged frame united by the negatively charged cloud of electrons. Corresponding transition of bonding is observed by means of electric conductivity as the *insulator-to-metal* or the *semiconductor-to-metal* types of melting.

In contrast to “normal” crystals, the glass-forming ones does not metallize at melting. Let us consider the crystals of chalcogen group – S, Se, Te as a simple example. Tellurium, being the non-glass-forming substance, is known to metallize continuously when heating above T_m [20], whereas glass-forming selenium and sulfur demonstrate the *semiconductor-to-semiconductor* transition [21] thus demonstrating conservation of covalent network in the molten state. This feature, which is known as the “polymeric” structure of glass-forming melts, does not explain, however, why covalent network becomes mobile after melting.

This puzzle can be resolved by means of alternative bonds and their wavelike self-organization as follows. A crystal of the glass-forming substance avoids metallization because of the low-temperature melting at $T_m < T_m^*$ (Fig.1, Table 1) owing to transformation of a piece of covalent bonds into the higher-energy alternative bonds accumulating excess thermal energy. Concentration of alternative bonds (AB) increases and reaches a critically high level when isolated can “feel” each other by local elastic fields generated in covalent network around each “alien” bond. For more and more effective accumulation of incoming thermal energy, alternative bonds gather into 2D layers, and then the layers organize into 3D bond wave representing the collectively moving layers populated with alternative bonds. Each step of AB self-organization means corresponding distortion of initial crystalline network, which destroys completely by 3D bond waves, whose wavefronts – the layers populated with alternative bonds continuously comb all the network in the wave direction.

Such a disappearance of crystalline order at melting does not mean, however, disappearance of order at all. Moreover, a rich *hierarchical* order appears. Let us illustrate this by means of Fig.2c which presents three different orders. The scale of *short-range order*, SRO, is defined by the length of covalent bond shown by short lines between white circles/atoms; this length is $l=2.3\text{\AA}$ for Se (Se-Se), 1.7\AA for SiO_2 (Si-O), etc. The SRO length can be extracted also from structural experiment as a radius of the *first coordination sphere*, $R_1 \approx 2\text{\AA}$, which is obtained by Fourier transformation of diffraction pattern.

The diffraction pattern itself gives information about the *medium-range order*, MRO, observed as the *First Sharp Diffraction Peak* (FSDP). The MRO length corresponds to the wavefront thickness $d=2\pi/Q_1 \approx 4-6\text{\AA}$, where Q_1 is the FSDP position. Equidistant wavefronts, two of which are shown in Fig.2c, give a relatively strong and *sharp* reflex. One can find other details about FSDP/MRO in my articles [12, 22-25].

The most intriguing is the *non-crystalline long-range order*, NC-LRO, in the form of Λ -lattice whose “elementary cell” one can see in Fig.2c. Unfortunately, Λ -lattice cannot be

detected by ordinary X-ray analysis ($\lambda=1-2\text{\AA}$) because of a strong parasitic scattering in the low- Q region; the synchrotron radiation of varying λ is an alternative. Fortunately, a simple indirect observation of Λ -lattices is possible just now by means of fractography, as it will be demonstrated in Section V, after Section III and Section IV which considers theoretical (III) and experimental (IV) aspects of the bond wave model.

III. ORDER PARAMETER – THE WAVELENGTH

Let us estimate the bond wave parameters as a function of temperature, beginning from concentration of alternative bonds

$$N = N_0 \cdot \exp(-\Delta\varepsilon/kT) \quad (1),$$

where $\Delta\varepsilon$ is the energy difference between the excited (AB) and the ground (CB) bonding states, and N_0 is a pre-exponent.

Of course, this approximation does not account interaction between alternative bonds, which, however, can be introduced by means of a simple geometry. From Fig.2c it follows

$$N/N_S = d/\Lambda \quad (2),$$

where N_S is the AB concentration in d -layer.

By combining of Eq.(1) and Eq.(2), one obtains the temperature dependence of the bond wave *wavelength*

$$\Lambda = \Lambda_3 = d \cdot (N_S/N_0) \cdot \exp(\Delta\varepsilon/kT) \quad (3).$$

Note that Λ_3 relates to the *three-dimensional* bond wave corresponding to region ‘I’ on the top part of Fig.3; other regions will be considered some later.

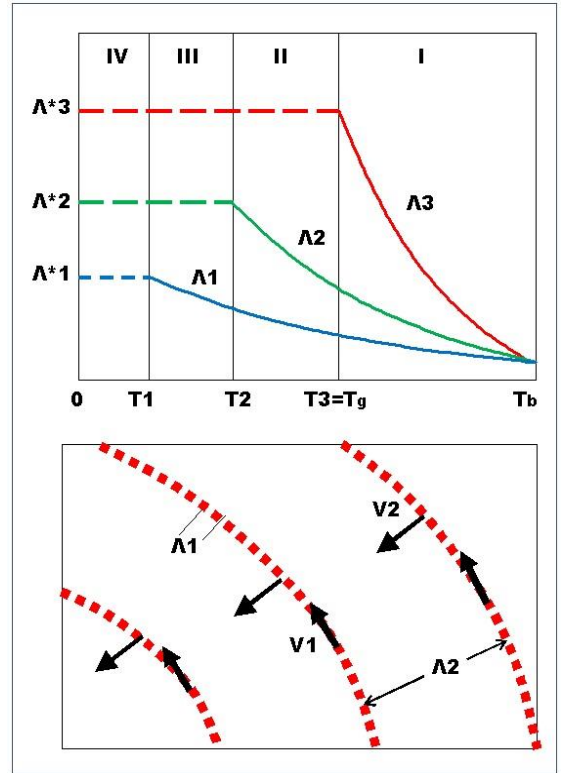


Figure 3. Temperature dependence of the wavelengths (top); 2D and 1D bond waves spreading along d -layer (bottom).

Bond wave dissipates thermal energy when moving through non-crystalline network with a temperature-dependent **velocity** $V(T)=f(T)\cdot d$, where $f(T)\sim\exp(-\varepsilon_f/kT)$ is frequency of the temperature activated “jumps” ($AB\rightarrow CB\rightarrow AB$, etc.), d is the wavefront thickness (**Fig.2c**), and ε_f is the jumping barrier. The reader can find numerical evaluation of $V(T)$ for Se in Ref.26. Despite of the same *exponential* temperature dependence for the bond wave velocity and wavelength, $\Lambda(T)$ and $V(T)$, they change in the *opposite* way. In addition, the velocity changes with temperature faster than wavelength because $\varepsilon_f > \Delta\varepsilon$ (barrier is higher than related levels).

When melt **heating**, the wavelength of 3D bond wave decreases up to a critical temperature when the wavefronts become in contact ($\Lambda_3=d$), so the network becomes homogeneous ($N=N_s$) and the bond wave disappears. This is a situation of **boiling**, when alternative bonds belonging to osculated wavefronts interact explosively with breaking and escaping of free covalent fragments into the gaseous phase.

In the opposite process of melt **cooling**, 3D bond wave reaches the second critical point, **T3**, when the critically distant wavefronts cannot “feel” each other by means of elastic field generated by them in surrounding covalent network. A feedback between the wavefronts breaks, and 3D bond wave stops, being *freezing* in the network in the form of Λ^*3 -lattice. As far as the *volume* mobility of a liquid is provided by the 3D bond wave, this freezing corresponds to **glass transition**; so $T_3=T_g$ and $\Lambda^*3=\Lambda_g$, as it is shown at the top part of **Fig.3**.

The 2D and 1D bond waves, representing respectively collective/mobile “strings” in the limits of each d -layer and collective alternative bonds in the limits of each string, remains refrozen below T_g , as it is shown in the bottom part of **Fig.3**. Nevertheless, these low-dimensional waves also freeze at related temperatures **T2** and **T1**. Below **T1** glass is completely “dead” in the sense that every mobility provided by the bond waves is arrested there.

Fortunately, the low-temperature “death” of glass is *reversible* owing to thermal generation of alternative bonds and their ability for integration. When **heating**, there refreeze successively 1D bond wave at/above **T1**, the 2D bond wave at/above **T2**, and finally the 3D bond wave at/above $T_3=T_g$. If the freezing/refreezing processes are not symmetrical (compare with braking/racing of a car), one can explain the phenomena of **hysteresis**, and not the well-known hysteresis around T_g (e.g., [8, p.29]) but also those at **T2** and **T1**. Corresponding two hysteresis can be detected when studying the low-temperature properties and/or the so-called “secondary relaxation” in glass.

As a result, four temperature regions can be distinguished:

Region I: Viscous liquid (T_g-T_b). All three bond waves (1D, 2D, 3D) coexist although the region specificity is determined by 3D bond wave that animates all the volume and thus appears in “macroscopic” processes, *viscous flow* first.

Region II: Plastic glass (T_2-T_g). Below $T_3=T_g$ concentration of alternative bonds in the frozen wavefronts remain high enough for realization of 2D bond waves which spreads along the stopped d -layers, thus providing 2D processes like *plastic flow* by sliding of d -layers under stress.

Region III: Brittle glass. Because of freezing of the 2D bond waves, glass enters the “brittle” region, when plastic flow and other 2D processes are arrested. A single response to mechanical stress is *destruction* of glass article, a fast process that denudes the frozen d -layers as the regions populated with a relatively weak alternative bonds; the jumping between the layers can be observed by characteristic *conchoidal fracture*.

Region IV: “Dead” glass. This hypothetical state is the most hard and immobile because of freezing of the bond waves of every dimension. Chaotic *explosive destruction* is expected.

IV. ATTRACTOR FOR THE VISCOSITY-TEMPERATURE BEHAVIOR

Let us begin from **Region I** which corresponds to viscous liquid. The well-known feature of glass-forming liquids is the *non-Arrhenius* behavior of viscosity, which is seen in **Fig.4a** even for GeO_2 , a typical “strong” liquid in terms of the strong-fragile classification after *Angell* [30].

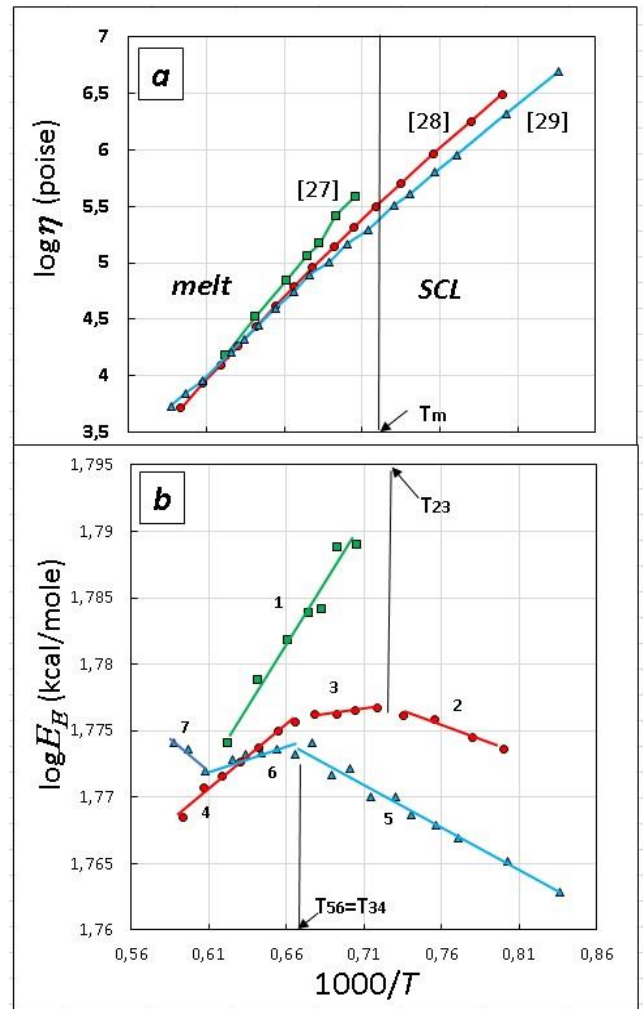


Figure 4. Experimental viscosity-temperature data for GeO_2 after *de Neufville et al* [27, Pt viscometer] (line 1), *Fontana & Plummer* [28, Run 1] (lines 2-4), and *Bruckner* [29] (lines 5-7) presented in the *Arrhenius* plot (a) and in the *TA*-plot (b).

Let call the *ideal strong liquid* a liquid that obeys the Arrhenius equation

$$\eta(T) = \eta_{\text{Arr}} \cdot \exp(E_{\text{Arr}}/RT) \quad (4)$$

with $\eta_{\text{Arr}} = \text{const}$ and $E_{\text{Arr}} = \text{const}$. For a real liquid, the both parameters are temperature dependent. To reduce the number of variables, we have used earlier [31] the Eyring equation [32]

$$\eta(T) = \eta_E \cdot \exp(E_E/RT) \quad (5).$$

Here only E_E , the *Eyring activation energy*, depends on temperature since the temperature dependence of $\eta_E = Nh/V$ (N and h are the Avogadro's and Plank's constants, and V is the molar volume) can be neglected because the temperature dependence of density, $\rho \sim 1/V$, is negligible as compared with that for viscosity. Typical glass-formers considered below have practically the same pre-exponent $\log \eta_E \approx -4$.

In this way, common two-factor analysis of the viscosity-temperature data by Eq.(4) can be substitute for the one-factor $E_E = f(T)$ analysis irrespectively of the liquid fragility, as it was demonstrated by me earlier [33]. The analysis includes three steps of an increasing generality.

1. TA plot $\rightarrow \Sigma\{A_i; G_i\}$

The first step begins from transformation of experimental $\eta(T)$ set into the $E_E(T)$ set by means of equations

$$E_E \text{ [kcal/mole]} = (4573/T) \cdot [\log \eta(T) - \log \eta_E] \quad (6)$$

$$\text{and } \eta_E \text{ [poise]} = 0.0039 \rho \text{ [g/cm}^3\text{]} / M \text{ [g]} \quad (7),$$

where ρ is average density and M is molecular weight; $\log \eta_E$ is equal to -4.0 for GeO_2 , -3.8 for SiO_2 , -3.65 for Se , etc.

The $E_E(T)$ points then brings into the $\log E_E(T) = 1/T$ plot similar to that shown in Fig.4b for GeO_2 , which is actually the “*twice activation*” (TA) plot because it is *activation* plot for *activation* energy. The TA-plot not only emphasizes the distinction between experimental $\eta(T)$ data from different sources (e.g., [27-29] in Fig.4a) but also elicits a new natural law described by equation

$$E_{Ei} = A_i \exp(G_i/RT) \quad (8).$$

Thus obtained lines of the $\{A_i; G_i\}$ parameters create a basis for the second analytical step.

2. Master plot $\rightarrow \{a; b\}$

Although the arrangement of TA-lines in Fig.4b looks chaotical, the $\{A_i; G_i\}$ pairs occur to relate as

$$\log A = a - b \cdot G \quad (9),$$

thus forming a *master line* like that shown in Fig.5 for GeO_2

The master line parameters, $\{a; b\}$, can be considered as **convergence point** whose coordinates defines all possible viscosity-temperature dependencies for the liquid considered. In terms of self-organization, convergence point represents the **attractor** for the viscosity-temperature behavior of a liquid.

In Table 2 there is a collection of convergence points for typical glass-formers, from strong to fragile, together with main

characteristics of glass-forming liquids including the value of viscosity at melting point, $\log \eta(T_m)$.

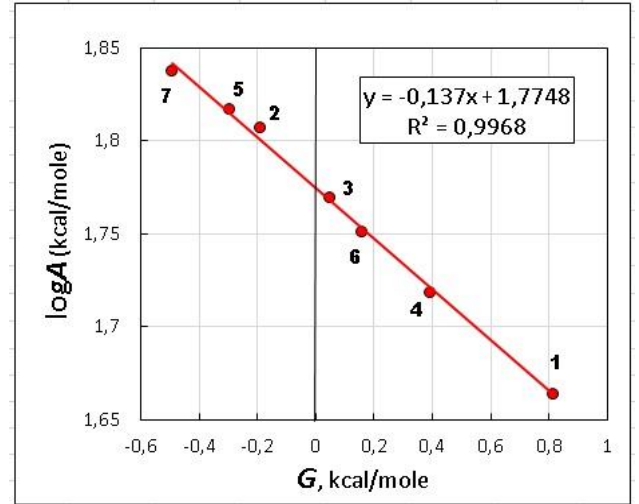


Figure 5. Master plot for GeO_2 . The point designation corresponds to the TA-lines in Fig.4b.

Table 2. Viscosity-temperature behavior for typical glass-forming liquids; fragility m by Eq.(11), η in [poise], a and b values are for [kcal/mole] dimension of A and G in Eq.(9).

Substance	T_g , K T_m , K	m $\log \eta(T_m)$	a b	Refs for $\{a; b\}$
SiO₂	1500	18	2.014	28, 29
	1983	7.8	0.101	
GeO₂	880	18	1.775	27-29
	1389	5.5	0.137	
B₂O₃	560	40	1.486	34
	748	4.8	0.298	
Se	310	55	1.324	35, 36
	494	1.6	0.700	
Gly	190	60	0.873	37, 38
	291	1.1	0.779	

Based on the existence of convergence point, one can formulate the **principle of partial reproducibility** for the viscosity-temperature experimental data:

viscosity of a liquid does not determined unambiguously by its temperature, the only one demand for the data correctness being their concordance with other measurements by fitting to the convergence point $\{a; b\}$ for the liquid considered.

This principle devaluates the ambition to obtain a “true” $\eta(T)$ dependence, as well as the attempts to construct the *general* equation for viscosity, a “Holy Grail” for generations of glass scientists. I propose instead the *universal* equation

$$\log \eta(T)_i = \log \eta_E + (A_i/2.303 RT) \cdot \exp\{[(a - \log A_i)/b]/RT\} \quad (10)$$

with a fixed $\{a; b\}$ and A_i varying along the liquid master curve in discrete manner.

3. Convergence plot $\rightarrow \Sigma\{a;b\}$

In **Table 2** it is seen that coordinates of convergence points change in the opposite direction and there is a relation between coordinates and the index of fragility defined as

$$m = |d(\log\eta(T)/d(T_g/T))|_{T_g} \quad (11).$$

These tendencies presented in **Fig.6**, distinguish two regions, the low- a region for “fragile” liquids (Se, glycerol) and the high- a region for “strong” liquids (GeO_2 , SiO_2), “intermediate” B_2O_3 being gravitating to the “strong” group.

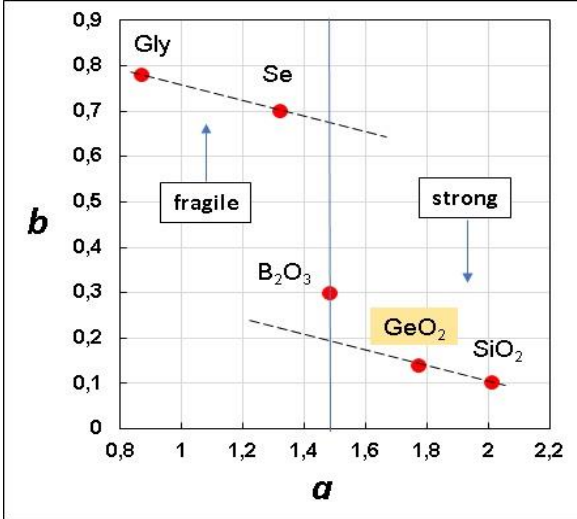


Figure 6. Convergence plot for the liquids in **Table 2**.

Investigation of convergence plot in more details will continue elsewhere, but now, in the context of self-organization, a possible mechanism by which a liquid selects one or another $\eta(T)_i$ from the permitted set is of interest. This is the problem of how adapts to its surrounding.

V. INFORMATION FIELD FOR THE BOND WAVE

A general instrument for adaptation of a self-organizing system is *information*, by which a feedback between the system and its medium realizes [39, 40]. Bond wave needs information about *direction* to move, therefore, an **information field** that gives this direction is a necessary condition for glass formation. Really, if the bond wave does not “know” where to run it cannot realize, so formation of a low-temperature melt ($T_m < T_m^*$ in **Fig.1**) is impossible.

Viscous flow proceeds in the temperature region of refrozen 3D bond wave which, being a dissipative pattern that animates all the volume of a sample, is the most adaptive state of the glass-forming substance. A possible mechanism for adaptation of a sample adapts to flow conditions during a real experiment is shown in **Fig.7**, where a sample successively selects viscous pattern by means of the **feedback loops** between the “substance” and “information” columns. So even the cooling/heating mode or the run number are significant, a fact that is clear for best experimentalists (see, e.g., [37] or [28]).

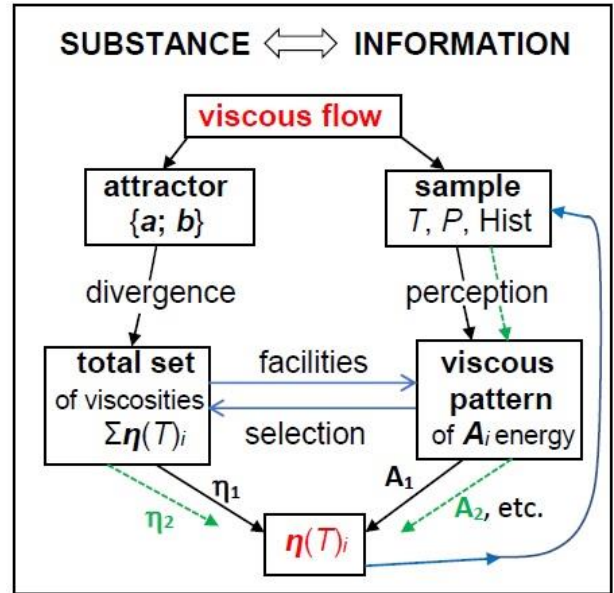


Figure 7. Self-organization at viscous flow of a sample depending on the sample chemical composition (substance), temperature (T), pressure (P), and history ($Hist$).

Although the main information field acting at viscous flow is the pressure gradient generated by viscometer (**gradP**), other information fields can coexist during the process. For example, a combined action of two information fields, pressure and temperature gradients (**gradP+gradT**), is shown in **Fig.8** using **fractography** as a simple method for observation of the frozen bond waves.

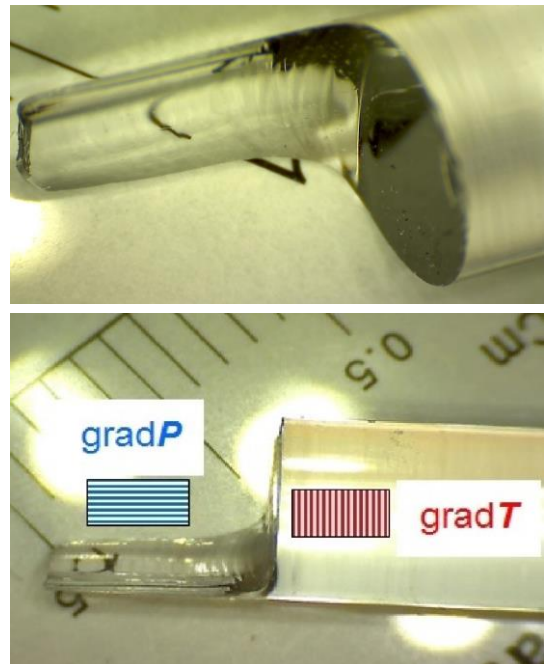


Figure 8. The fractured glassy rod (see text for details).

To draw a glassy rod from a softening ingot, one uses two gradients: the temperature gradient (*gradT*) from a heater and the pressure gradient (*gradP*) from a drawing device. The fracture in **Fig.8** elicits both waves by their Λ -lattices frozen in solid glass. A remarkable feature of this fracture is the *solitonic* behavior of underlaying bond waves, as far as solitons are defined as the waves intersecting without distortion. Although information fields were acting independently here, such behavior is not the case for our experiments listed in **Table 3**.

Table 3. The field effects studied in our laboratory; $=\mathbf{H}$ and $\sim\mathbf{H}$ correspond to constant and pulsed magnetic field, **US** correspond to ultrasonic field in the cavitation regime.

IF	Substance	Property	General effect	Ref.
$=\mathbf{H}$ 240Oe	Se	Viscosity (in situ)	$\Delta\lg\eta^H=\pm 0.2$ <i>Anisotropy</i>	[6]
$\sim\mathbf{H}$ 240Oe, 50 Hz	Se	Viscosity (in situ)	Resonance $\Delta\lg\eta^H=+0.3/-0.5$ <i>Anisotropy</i>	[7]
$=\mathbf{H}$ 240Oe	As ₂ S ₃	Color Fracture	<i>Red shift</i> for the “magnetic” sample (MS); <i>Plane fracture</i> (MS in Fig.9)	[41]
US 0.3 W/cm ²	Se-Te	Optical trans- mission spectra.	<i>Non-linear</i> change in Se-X series of glasses; <i>Anisotropy</i> .	[42]
	Se-As			[43]
	Se-S	SEM	Unusual images;	[44]
	Se:Cl		<i>Anisotropy</i> (Fig.11 ; Se-Te)	[45]

First series of experiments on *viscous flow* of softening Se glass in **magnetic field** [6,7] was initiated by *Dembovsky* in his search for “glassy” bonds that provides switching of covalent bonds by means of charged intermediate states [4]. It was proposed that magnetic field can interact with electric current due to collective switching at viscous flow, so influencing on viscosity.

Although the expected effect in **constant** magnetic field was really observed [6], there were two problems that hampered the effect recognition. First, common glass like Se is the *diamagnetic* material – even the defects are considered to be diamagnetic in the basic state. Second problem is *weakness* of the applied field, whose energy is negligible as compared with thermal energy ($\mu_B H \ll kT$), so the magnetic field cannot interact with the proposed current, even if it exists.

Of course, the obtained effect would be presented as an experimental fact that needs further theoretical explanation, if not a relatively low value of the effect, $|\Delta\lg\eta| \approx 0.2$, which can be easily attributed to experimental error. A simple way of increasing the field intensity for increasing the effect value was forbidden for us technically. Therefore, we changed the

not the field intensity but the field character by using a **pulsed** magnetic field of the **50 Hz** frequency.

The pilot experiment at few temperatures showed no the magnetic field influence. However, after a detailed scanning of temperature, a new phenomenon of the **magneto-viscous resonance** was revealed, when in a narrow region at **321K** a strong effect, $|\Delta\lg\eta^H| \rightarrow 0.5$, was obtained [7].

To understand the magneto-viscous effects of both constant and pulsed fields, we have proposed first the existence of *one-electron* transition state B^* which arises at the elementary act of bond exchange ($CB \leftrightarrow B^* \leftrightarrow AB$) [46]. Then magnetic field interacts with not the previously proposed electric current but with paramagnetic states B^* accompanying the process of switching of covalent bonds at viscous flow.

The *resonance* character of the effect indicates that frequency of thermally-activated acts of bond exchange coincides with the field frequency [46]. However, the problem of the field weakness remained. To overcome it, I have proposed that the B^* -jumps are correlated not only in time by the temperature dependent frequency but also in space. In this moment the bond wave model was born, together with the information field concept.

In the magneto-viscous experiments there are two information fields, *gradP* and \mathbf{H} . To consider the magnetic field only, the “magnetic/non-magnetic” pairs of Se, As₂Se₃ and As₂S₃ glasses were prepared in 1984 [47]. The case of As₂S₃ was especially interesting because of unusual color of the “magnetic” sample, which changed natural red color to almost black, as it is shown in **Fig.9**. The second difference has emerged ten years later, when I have splitting these samples for presentation in the MRS conference [41]. The cylindrical samples were splatted in the middle by a knife blade – the blow direction is shown by white arrows.

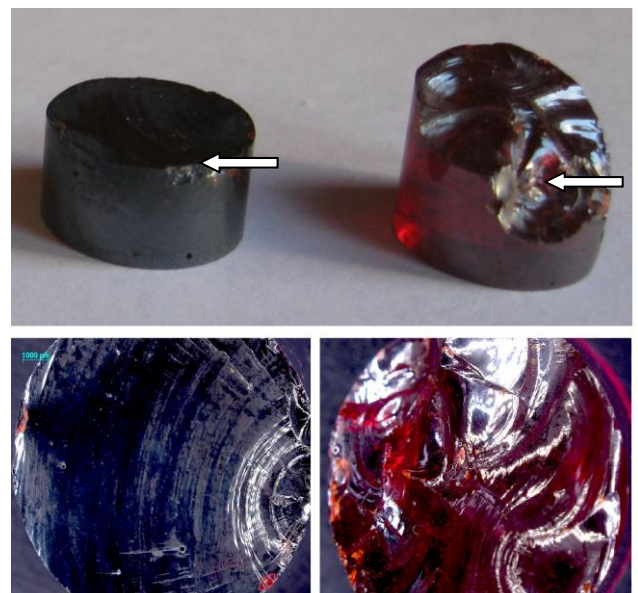


Figure 9. The fractured samples of “magnetic” (on the left) and “non-magnetic” (on the right) As₂S₃ glasses; a sight from sideways (top) and from above (bottom).

To understand both differences, one should consider the details of experiment. “Non-magnetic” and “magnetic” samples were prepared under the same conditions, namely, by melting of industrial As_2S_3 in evacuated quartz ampules at 450°C for 1 hour in a tube furnace placed inside electromagnet, with the following 20 min cooling inside the cutting off furnace up to room temperature. The field of 240 Oe was acting on the “magnetic” sample *during the melting/cooling process*.

On the first glance, the features observed in “magnetic” sample conflict with the bond wave model. Really, as far as the *transversal* field of electromagnet orients the wavefronts *across* the tube/sample axis, the fracture should develop *along* the sample, in contrast to that observed in left-top corner of **Fig.9**. Besides, the darkening of “magnetic” sample remains a puzzle. The bond wave model resolves it when considering the bond wave dimensionality.

In accord with the top part of **Fig.3**, the bond waves of all three dimensions (1D, 2D, 3D) realize when treating the samples at temperatures above T_g . General dynamic factor here is the 3D bond wave which animates all the structure by its wavefronts representing *d*-layers populated with alternative bonds. As far as the acts of bond exchange through paramagnetic intermediate state are oriented by magnetic field, 3D bond wave runs in the field direction, and *d*-layers orient *along* the ampule/sample axis.

A critical situation appears when approaching T_g , when the 2D bond waves (the families of strings moving collectively along each *d*-layer – see the bottom part of **Fig.3**) become main dynamic factor. Now magnetic field acts mainly on the strings, which therefore *turn* their *d*-layers in the freezing network. The fracture observed in “magnetic” sample indicates that the strings have completed **rotation** of *d*-layers before total solidification of the sample.

The observed darkening of “magnetic” sample follows from this rotation. Those working in the field of glassy semiconductors are well-acquainted with the *red-shift* of optical edge observed after low-temperature illumination of chalcogenide amorphous films. We have proposed earlier an explanation of this phenomenon as a loosening of covalent network due to the light-induced drift of three-center bonds (hypothetical alternative bonds) [48]. By analogy, the red-shift observed in “magnetic” As_2S_3 can be explained by loosening of the solidifying covalent network due to the field-induced rotation of *d*-layers.

Finally, let consider a complex fracture of “non-magnetic” sample shown in the right part of **Fig.9**. The form of fracture reflects unstable thermal field $\Sigma \text{grad}T$ that was realizing during solidification. Then a plane cross-fracture of “magnetic” sample in **Fig.9** indicates that magnetic field has won the “information battle” between $\Sigma \text{grad}T$ and **H**.

Last experiment concerns **ultrasonic** (US) field, which was applied in the *cavitation* regime to softening Se-X glasses ($X = \text{Te}, \text{S}, \text{As}, \text{Cl}$) with Se as the main component. Fresh samples displayed a strong **non-linearity** observed in the form of extremum on the concentration-property curves at 1-2%Te, 5%As, 1%S, and 0.01-0.02%Cl [49]. Owing to a low glass-transitions temperature of the samples ($T_g \approx 40^\circ\text{C}$ for Se), a

simple cell (**Fig.10**) with water as cavitation medium was used. The treatment temperatures are 40°C , 50°C , and 72°C ; the treatment time is some minutes (2-5 min depending on temperature); the field intensity is about 0.3 W/cm^2 .

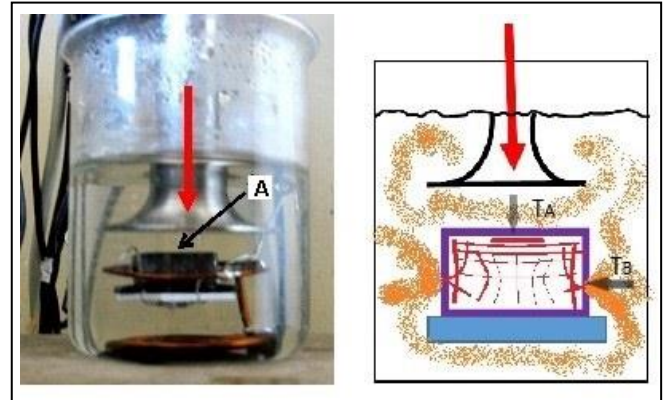


Figure 10. US-treatment of Se-X samples: the cell (on the left) and the scheme of interaction (on the right). Red arrow is the US input, red curves are the wavefront section. Arrows T_A and T_B indicate two directions for measurement of optical spectra.

The samples of a given Se-X series were measured by optical transmission spectra in the $300\text{-}5000 \text{ cm}^{-1}$ range before and after each treatment. Specific lines and *transparency*, T , (optical transmission at the 1000 cm^{-1} , a frequency that divides vibrational region and the “window of transparency” for selenide glasses) was watched during experiment. Since there was no change in spectra of Se standard hold in water of 72°C for 5 minutes when the US transmitter was turned off, one can attributed the observed effects just to the US influence.

Let us consider the most remarkable features of the cavitation effects including the non-linear response using **Fig.11**. There are two final samples from the same Se-Te series; the fractures are parallel (**B**) or perpendicular (**A**) to the US-input indicated in **Fig.10** by thick red arrows.

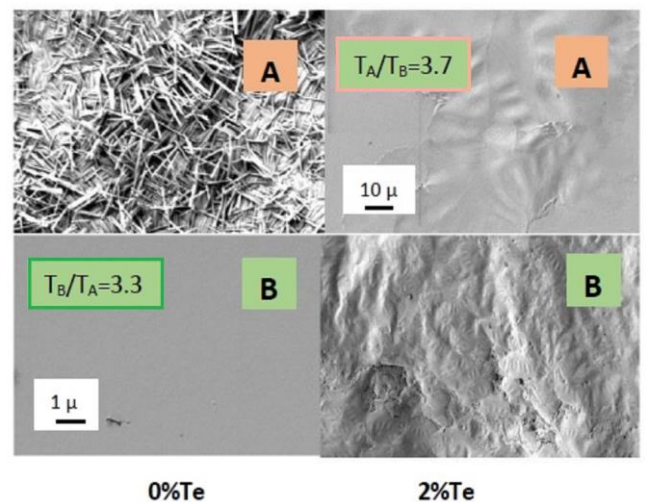


Figure 11. SEM images of fractured Se and $\text{Se}_{98}\text{Te}_2$ samples.

Two samples in **Fig.11** belong to the 0-1-2-5-10%Te series, the 0%Te (pure Se) being a “normal” member while the 2%Te being an “extremal” one because it fits in the 1-2%Te region of non-linearity. Transparency became very low after final 72°C treatment, nevertheless, the measured values indicate clearly *optical anisotropy* and, moreover, the anisotropy *inversion*: from $T_A < T_B$ for “normal” Se to $T_A > T_B$ for “extremal” 2%Te. Note that before US-treatments all glasses were normally isotropic ($T_A = T_B$) and of the same transparency.

Although all fractures looked glassy by the eye (smooth and bright), the SEM images were not, except lateral fracture of pure Se (**B**-fracture for 0%Te in **Fig.11**). The difference in transparency of the samples measured in frontal (T_A) and lateral (T_B) directions ($T_B/T_A = 3.3$ for 0%Te and $T_A/T_B = 3.7$ for 2%Te) coincides with their SEM images, when the observed inhomogeneities act as light scatters. The problem is their unusual form. The *needles* on the **A**-fracture of Se (0%Te) look like microcrystals, however, Se is known to crystallize in the *spherulitic* manner. The *clouds*, which are observed on the both fractures of 2%Te sample, look neither crystalline nor glassy, being probably an intermediate *glass-to-crystal* form arising due to cavitation treatment of this “extremal” sample.

The problem is that we do not know *when* the observed “needles” and “clouds”, were formed: *during* cavitation treatment or *after*, when the samples were cooling and/or when keeping before SEM. The last variant has emerged due to repeat SEM of Se (0%Te) after 6 months: the needles have appeared on the **B**-fracture too, although not as a carpet but as a family of needle islands. This shows that the cavitation-induced crystallization continues in solid glass, which therefore remains in an activated state even below T_g . In every case, the *low-temperature* ($T < T_g$) crystallization, as a process provided by 2D bond waves, should differ from the *high-temperature* ($T > T_g$) crystallization realized by means of 3D bond waves. The difference is not only in kinetics but also in morphology and in the volume-or-surface location [50].

VI. DISCUSSION

The proposed approach to glassy state differs from conventional one in basic points indicated in **Table 4**. Let us consider the difference in frames of four topics usually discussed by glass community – from structure and properties to glass transition and practical usage.

1. Structure. Common definition of glass as “a solid having no long-range order” means not more than “glass is not a crystal” when common *crystal*-type long-range order (LRO) is meant as usual. Bond wave creates a specific *non-crystalline LRO* that coexists naturally with the medium-range order (MRO) and the short-range order (SRO) [51]. Corresponding scales are the wavelength Λ for NC-LRO, the wavefront thickness d for MRO, and the covalent bond length l for SRO (see **Fig.2c** for visualization).

When cooling of supercooled liquid at/below T_m , there appears a *competition* between 3D bond wave supporting NC-LRO and a tendency to establish “normal” crystal-type LRO. Formation of glass means that 3D bond wave has won the battle of orders.

Table 4. Glass paradigms reconsidered.

GLASS	Conventional notions	The Bond Wave model
Long-Range-Order	Absent	NC-LRO in the form of Λ -lattice
Chemical Bonding	One-state: covalent bond	Two-state: $CB \leftrightarrow AB$
Reproducibility at $T > T_g$	Total, depending on temperature	Partial, depending on glass history
Glass Transition	Various models and theories	3D BW \rightarrow 2D BW transition at T_g
Glass Structure	Models/theories based on CRN	Hierarchical: SRO/MRO/NC-LRO
Management of Properties by...	...Chemical Composition	...Composition and Information Fields
Glass Definition	Non-crystalline solid obtained by cooling from melt at a sufficiently high rate (critical cooling rate)	Non-crystalline solid obtained from a liquid possessing self-organization ability in the form of the bond waves

Abbreviatures: CB – covalent bond, CRN – continuous random network, NC-LRO – non-crystalline long-range order, AB – alternative bond, BW – bond wave, MRO – medium-range-order (known also as IRO – intermediate range order).

2. Reproducibility. Supercooled liquid that exists in the $T_g < T < T_m$ range is assumed to be in the “metastable equilibrium”, a term that implies a definite property-temperature relation. Then every appreciable deviation from a “true” property-temperature dependence is scarified as “experimental error”. It was demonstrated in Section IV that the viscosity-temperature behavior of glass-forming liquids does not determined strictly, being possessing a *freedom* which is restricted only by *convergence point* of the liquid – or *attractor* in terms of self-organization.

One may expect similar attractors for other temperature dependent properties. As to the viscosity attractor, it generates a family of *viscous patterns* which represents themselves as lines in the twice-activation coordinates. The observed transition between the patterns at T_{ij} can be compared with the “liquid-liquid” phase transitions (see [52] for introduction), although this is a far analogy for at least two reasons. First, the transition between viscous patterns looks rather chaotic (like 1-7 lines in **Fig.4b**), being depending not only on temperature but also on the sample history (**Fig.7**). Second, if one interprets the $\eta(T)_i$ viscous pattern as a “phase”, this is the *dynamic* phase transition observed under *normal pressure*. The pressure-induced shift of convergence point will be considered in my next paper.

3. Glass Transition is a central point in glass science, being also an object of a permanent discussion for more than century. Main disagreement concerns the nature of a dramatic

loss of mobility below T_g , the glass transition temperature. In frames of the bond wave model, glass transition is the **dimensionality** one: from 3D BW in liquid to 2D BW in solid. As far as 3D bond waves are frozen/stopped below T_g , the *volume* mobility, including viscous flow, is arrested below T_g , where only the low-dimension processes, such as plastic flow along the stopped *d*-layers, remain. This is my answer to the principal question “*why glasses do not flow*” [53]. As to the numerous theories/models of glass transition proposed so far, I know the only one that also uses dimensionality – this is the *Ojovan* model for silica which considers a hypothetical system of percolating clusters named “vitrons” [54]. This model, however, leads to the *increase* of dimensionality when cooling – from fractal dimensionality $d_f=2.3$ in liquid to Euclidian dimensionality $d=3$ in glass.

4. Practice. It is quite evident that development of technology needs a deeper understanding of the processes implicated. With the bond wave model, there appears a possibility for reasonable usage of the low-energy **information fields** to improve the glass making process. Note that information fields just present at the process, at least in the form of temperature and pressure gradients (**gradT+gradP**), and one can use them more effectively based on the underlying bond wave picture.

Besides common temperature/pressure gradients, one can introduce other information fields, e.g., *magnetic* and *ultrasound* fields (**H** and **US**), whose influence on softening **bulk** glasses was demonstrated in Section V. Applicability of the bond wave model to thin **films** was demonstrated in Ref.55 on the example of memory elements based on the electric switching phenomenon (*electric* information field) and microlenses formed under laser illumination (*electromagnetic* information field).

When using information fields, one should take in mind two implications. First, external field can provide both *energy* – for the bond wave support, and *information* – for giving the wave direction. A simple example is the thermal field of a given intensity (temperature, the energy level) and direction (temperature gradient, information). Second, there are usually two or more potential information fields, which can *coexist* in the solitonic manner (see **gradT** and **gradP** in **Fig.8**), *interact* (as **gradP** and **H** in our magneto-viscous experiments), and *depress* a competitor (**H** has eliminated **gradT** in the “magnetic” sample – **Fig.9**). Besides, a post-action of information field is possible (see the last comment to **Fig.11**).

VII. CONCLUSIONS

A new approach to glassy state, which combines classical **self-organization** and the **chemical bond** theory in the context of “glassy” bonds after S. A. Dembovsky (1932-2010), is proposed. This approach is realized in the form of the **bond wave model** which, with the use of available experimental data, leads to nontrivial notions about (1) **non-crystalline long-range order**, (2) **partial reproducibility** of experimental data, and (3) **information fields** as a necessary condition for glass formation and a perspective instrument for management of glass properties.

The bond wave model concentrates now on the wavefronts, i.e., on a relatively small (but exceptionally active!) piece of non-crystalline structure. As far as the wavefronts pass continuously through every point/atom of a network, the “**secondary**” **self-organization** develops in the most of structure; in this way a link between the “*topological*” and the “*bond wave*” aspects of self-organization appears.

REFERENCIES

- [1] H. Haken. Synergetics. An Introduction (3rd ed). Springer, Berlin-Heidelberg, 1983.
- [2] I. Prigogine. From Being to Becoming. Freeman, San Francisco, 1980.
- [3] W. Zhang. Selforganizology: The Science of Self-Organization. World Sci. Publ., Singapore, 2015.
- [4] S. A. Dembovsky. The connection of quasidefects with glass formation in the substances with high lone-pair electron concentration. Mater. Res. Bull. 16 (1981) 1331.
- [5] S. A. Dembovsky, E. A. Chechetkina. Glassy materials clarified through the eyes of hypervalent bonding configurations. J. Optoe. Adv. Mater. 3 (2001) 3.
- [6] S. A. Dembovsky, S. A. Kozyukhin, E. A. Chechetkina. The experimental observation and investigation of defects in glass forming substances with selenium as an example by viscometry in magnetic and electric fields. Mater. Res. Bull. 17 (1982) 801.
- [7] S. A. Dembovsky, E. A. Chechetkina, S. A. Kozyukhin. Anomalous effect of weak magnetic fields on diamagnetic glassy semiconductors. JETP Lett. 41(1985) 88.
- [8] J. Zarzycki. Glasses and the Vitreous State. Cambridge University Press, Cambridge, 1991.
- [9] A. K. Varshneya. Fundamentals of Inorganic Glasses (1st ed.). Academic Press Inc., 1993.
- [10] W. H. Zachariasen. The atomic arrangement in glass. J. Amer. Chem. Soc. 54 (1932) 3841.
- [11] H. A. Robinson. On the structure of vitreous SiO₂ – I. A accounting new pentagonal dodecahedral model. J. Phys. Chem. Solids 26 (1965) 209.
- [12] E. A. Chechetkina. Is there a relation between glass-forming ability and the first sharp diffraction peak? J. Phys.: Cond. Mat. 7 (1995) 3099.
- [13] Z. Shemer, V. Halpern. Correlated weak bonds as a source of the Bozon peak in glasses. (2006) arXiv: 0604714v1.
- [14] J. C. Phillips. Realization of a Zachariasen glass. Solid State Comm. 47 (1983) 203.
- [15] P. Boolchand, G. Lucovsky, J. C. Phillips, M. F. Thorpe. Self-organization and the physics of glassy networks. Philos. Mag. 85 (2005) 3823.
- [16] J. C. Mauro. Topological constraint theory of glass. Amer. Ceram. Soc. Bull. 90 (2011) 31.
- [17] M. Bauchy. Topological constraint theory and rigidity of glasses. (2020) arXiv: 2005.04603.
- [18] P. Boolchand, D. G. Georgiev, B. Goodman. Discovery of the intermediate phase in chalcogenide glasses. J. Optoe. Adv. Mat. 3 (2001) 703.

- [19] E. A. Chechetkina. Rawson's criterion and intermolecular interactions in glass-forming melts. *J. Non-Cryst. Solids* 128 (1991) 30.
- [20] A. S. Epstein, H. Fritzsche, K. Lark-Horovitz. Electrical properties of tellurium at the melting point and in the liquid state. *Phys. Rev.* 107 (1957) 412.
- [21] A. M. Regel, V. M. Glazov. Physical properties of electronic melts. (in Russ.) Nauka, Moscow, 1980.
- [22] E. A. Chechetkina. The first sharp diffraction peak in glasses and the other amorphous substances. *J. Phys.: Cond. Mat.* 5 (1993) L527.
- [23] E. A. Chechetkina. Synergetic model for the first sharp diffraction peak in amorphous substances. *Solid State Comm.* 87 (1993) 171.
- [24] E. A. Chechetkina. Medium-range order in amorphous substances: A modified layer model. *Solid State Comm.* 91 (1994) 101.
- [25] E. A. Chechetkina. Self-organization in glass: The synergetic chemical bonding approach. *J. Optoe. Adv. Mater.* 18 (2016) 44.
- [26] E. A. Chechetkina. Glassy State Clarified from the Eyes of Self-Organization. Amazon Kindle Direct Publishing, 2019.
- [27] J. P. de Neufville, C. H. Drummond III, D. Turnbull. The effect of excess Ge on the viscosity of GeO₂. *Phys. Chem. Glasses* 11 (1970) 186.
- [28] E. H. Fontana, W. A. Plummer. A study of viscosity-temperature relationships in the GeO₂ and SiO₂ systems. *Phys. Chem. Glasses* 7 (1966) 139.
- [29] R. Bruckner. Physikalische Eigenschaften der oxydischen Hauptglasbildner und ihre Beziehung zur Struktur der Gläser: I. Schmelz- - und Viskositätsverhalten der Hauptglasbildner. *Glastechn. Ber.* 37 (1964) 413.
- [30] C. A. Angell. Relaxation in liquids, polymers and plastic crystals – strong/fragile patterns and problems. *J. Non-Cryst. Solids* 157 (1991) 131.
- [31] E. A. Chechetkina, S. A. Dembovsky. On the form of the viscosity-temperature dependence for glasses and their melts. *J. Non-Cryst. Solids* 105 (1988) 171.
- [32] H. Eyring. Viscosity, plasticity and diffusion as examples of absolute reaction rates. *J. Chem. Phys.* 4 (1936) 283.
- [33] E. A. Chechetkina. Key distinctions in activation parameters of viscous flow for 'strong' and 'fragile' glass-forming liquids. *J. Non-Cryst. Solids* 201(1996)146.
- [34] T. J. M. Visser, J. M. Stevels. Rheological properties of boric oxide and alkali borate glasses. *J. Non-Cryst. Solids* 7 (1972) 376.
- [35] S. V. Nemilov, A. O. Ivanov. Viscosity of Se-Ge glasses in the softening range. *Zh. Prikl. Khim.* (J. Appl. Chem., in Russ.) 36 (1963) 2541.
- [36] S. A. Kozyukhin. Rheological properties of selenium and selenium-tellurium in the metastable liquid region. Diss. thesis, Inst. Gen. Inorg. Chem., Moscow, 1991.
- [37] R. L. Cook, H. E. King, Jr., C. A. Herbst, D. R. Herschbach. Pressure and temperature dependent viscosity of two glass-forming liquids: glycerol and dibutyl phthalate. *J. Chem. Phys.* 100 (1994) 5178.
- [38] G. Tammann, W. Hesse. The dependence of viscosity upon the temperature of supercooled liquids. *Z. anorg. Allgem. Chem.* 156 (1926) 245.
- [39] H. Haken. Information and Self-Organization. A Macroscopic Approach to Complex Systems. Springer, Berlin-Heldenberg, 2006.
- [40] H. Haken, J. Portugali. Information and Selforganization: A Unified Approach and Applications. *Entropy*, 18 (2016) 197.
- [41] E. A. Chechetkina. Fracture and fractals in glasses. In: *Fractal Aspects of Materials*, MRS Proc. 367 (1995). P.397-403.
- [42] E. A. Chechetkina, E. V. Kisterev, E. B. Kryukova, A. I. Vargunin. Crystallization of Se-Te glasses in ultrasonic field. *J. Optoe. Adv. Mat.* 11 (2009) 2029.
- [43] E. A. Chechetkina, E. V. Kisterev, E. B. Kryukova, A. I. Vargunin. Crystallization of Se-As glasses in ultrasonic field according to the optical transmission data. *Inorg. Mater.: Appl. Res.* 2 (2011) 311.
- [44] E. A. Chechetkina, E. V. Kisterev, E. B. Kryukova, A. I. Vargunin, S.A. Dembovskii. Preparation of chalcogenide glass-ceramic materials by ultrasonic treatment of glasses. *Inorg. Mater.: Appl. Res.* 3 (2012) 11.
- [45] E. A. Chechetkina, E. V. Kisterev, E. B. Kryukova, A. I. Vargunin. Influence of ultrasound on crystallization of Se:Cl glasses. *Materialovedenie* (Russ.) No.12 (2012) 3.
- [46] S. A. Dembovsky, E. A. Chechetkina. Resonance phenomena and defects in amorphous selenium. *Philos. Mag.* B53 (1986) 367.
- [47] E. A. Chechetkina, S. A. Dembovsky, *et al.* Influence of weak magnetic and electric fields on structure of chalcogenide glassy semiconductors. In: *Proc. "Amorphous Semiconductors-84"*, Gabrovo, 1984.88-90.
- [48] S. A. Dembovsky, E. A. Chechetkina. Hypervalent bonds as active centers providing photo-induced transformations in glasses. In: *Photo-Induced Metastability in Amorphous Semiconductors* (ed. A.V. Kolobov). Wiley-VCH, Weinheim, 2003. P.299-310.
- [49] S. A. Dembovsky, E. A. Chechetkina, T. A. Kupriyanova. Non-linear influence of impurities on the properties of glassy selenium. *Materialovedenie* No.4 (2004) 37.
- [50] E. A. Chechetkina. Crystallization in glass-forming substances: The chemical bond approach. In: *Crystallization: Science and Technology* (ed. M.R.B. Andreetta). InTech, Croatia, 2012. P.3-28.
- [51] E. A. Chechetkina. The shape of order in glasses. *Phys. Stat. Sol.* B49 (2012) 2034.
- [52] S. M. Stishov. Melting and polymorphic transitions in liquid. (2024) arXiv :2404.12392v1.
- [53] J.-P. Bouchaud. Why the dynamics of glasses super-Arrhenius? (2024) arXiv :2402.01883v2.
- [54] M. I. Ojovan. Glass formation in amorphous SiO₂ as a percolation phase transition in the system of network defects. *JETP Lett.* 79 (2004) 769.
- [55] E. A. Chechetkina. Photostructural changes and electrical switching in amorphous chalcogenides: Bond waves in thin films. *Nat. Sci.* 10 (2018) 70.